Supporting Informations

Structural Advantage of Keto-Linked Fe-Porphyrin Polymer in Boosting Hydrogen Evolution Reaction

Xiaoyu Zhai[a], Kainan Wang[a], Cheng Yuan[a], Pengfei Chen[a], Aijian Wang[*,a], Jun Qian[a], Long Zhao[a], Weihua Zhu[a], Danhong Shang[b]

[a]School of Chemistry & Chemical Engineering, Jiangsu University, Zhenjiang 212013, P.R. China

[b]School of Environmental and Chemical Engineering, Jiangsu University of Science and Technology, Zhenjiang 212013, PR China

Corresponding Author. Tel: +86-511-88791928. E-mail: wajujs@ujs.edu.cn

Experimental section

Reagents and Materials

All chemical reagents employed in this investigation were of analytical grade and were acquired from commercial sources without further purification, unless explicitly stated otherwise. Specifically, anhydrous ferric chloride ($FeCl_3$), nickel chloride ($NiCl_2$), methanol (CH_3OH), 2,4,6-triformylphloroglucinol (Tp) and tetrahydrofuran (THF) were obtained from Shanghai Sinopharm Chemical Reagent Co., Ltd. The key organic precursor 5,10,15,20-tetrakis(4-aminophenyl)porphyrin (TAPP), was synthesized in our laboratory following previously reported methods with appropriate modifications to optimize the synthetic procedures.[17] High-purity deionized water (18.2 MΩ·cm at 25 ^{o}C), produced by a Millipore Milli-Q Integral water purification system, was utilized throughout all experimental procedures, including material preparation, characterization, and electrochemical measurements, to ensure consistency and reproducibility.

Material Characterizations

The structural and morphological characteristics of the synthesized materials were systematically investigated using a comprehensive suite of characterization techniques. Surface morphology and elemental composition were analyzed by field-emission scanning electron microscopy (FE-SEM, S-7800, Hitachi) coupled with energy-dispersive X-ray spectroscopy (EDS) at an accelerating voltage of 15 kV. Chemical states and surface composition were determined by X-ray photoelectron spectroscopy (XPS) using an ESCALAB 250XI system (Thermo Fisher Scientific) with monochromatic Al Kα radiation (hν = 1486.6 eV). Fourier transform infrared (FTIR) spectroscopic analysis was conducted on a WQF-410 spectrometer (Ruili Analytical Instrument Co., China) using KBr pellets, with spectra collected in the range of 500-4000 cm^{-1} at a resolution of 4 cm^{-1}. Optical properties were evaluated through UV-vis absorption spectroscopy using a JASCO V-570 spectrophotometer (Shimadzu Corporation, Japan), with measurements performed in dimethyl sulfoxide (DMSO) solvent across the wavelength range of 300-1100 nm. Textural properties, including specific surface area and pore size distribution, were determined by nitrogen adsorption-desorption isotherm measurements at 77 K using a Micromeritics TriStar II 3020 surface area and porosity analyzer, with samples degassed at 120 ^{o}C for 12 h prior to measurement.

Electrochemical Measurements

All electrochemical experiments were conducted using a CHI614E electrochemical workstation (Chenhua, Shanghai) with a 1.0 M KOH solution as the electrolyte. A Hg/HgO electrode and a graphite rod served as the reference and counter electrodes, respectively. The working electrode was prepared through a series of steps. Specifically, 4 mg of the sample powder was dispersed in a mixture of 400 μL ethanol and 20 μL Nafion (5 wt%) within a 1 mL centrifuge tube to form a homogeneous ink. Subsequently, 100 μL of the catalyst ink was drop-cast onto a pre-cleaned nickel foam (1 × 1 cm^2) and dried at 60 ^{o}C for 30 min under vacuum. All measured potentials were converted to values relative to the reversible hydrogen electrode (RHE) using the Nernst equation. Considering the potential surface passivation of the samples upon air exposure, cyclic voltammetry (CV) was initially performed to activate the materials, with electrochemical measurements commencing only after the CV curves achieved a stable, reproducible profile [20]. Linear sweep voltammetry (LSV) measurements were conducted in a potential window of -0.8 to -1.6 V vs RHE in 1.0 M KOH electrolyte. To thoroughly characterize the electrochemical behavior, CV measurements were systematically performed at varying scan rates (20, 40, 60, 80, and 100 mV s^{-1}). The electrochemical double-layer capacitance (C_{dl}), which serves as a critical parameter for determining both the catalytic active sites and electrochemical active surface area (ECSA), was quantified through CV measurements at multiple scan rates in 1.0 M KOH (pH = 14). Electrochemical impedance spectroscopy (EIS) analysis was conducted in a broad frequency range (10^{-2} to 10^{6} Hz) to investigate the charge transfer characteristics during the HER process. The long-term electrochemical stability of Tp-FeTAPP in alkaline media was rigorously assessed through an extended period of continuous operation, with the evolved hydrogen quantified by gas chromatography to determine the Faradaic efficiency with high precision.

Synthesis of Tp-MTAPP polymers

A certain amount of TAPP (65 mg) and Tp (80 mg) were dissolved in 30 mL of methanol in a 50 mL round-bottom flask (Scheme 1). The solutions were then combined and subjected to ultrasonic treatment for 40 min to ensure uniform dispersion. The mixture was subsequently heated at 75 °C for 48 h. After cooling to room temperature, the resulting products were filtered, washed several times with deionized water, and dried at 60 °C under vacuum for 12 h, yielding Tp-TAPP as a black powder precursor. To synthesize Tp-FeTAPP, 50 mg of Tp-TAPP precursor and 188 mg of anhydrous $FeCl_3$ were precisely weighed and transferred into a 100 mL three-neck round-bottom flask containing 30 mL of anhydrous THF. The mixture was subjected to ultrasonic dispersion (40 kHz, 300 W) for 30 min to achieve a homogeneous suspension. Subsequently, the reaction system was maintained at 80 °C under continuous magnetic stirring for 48 h in an oil bath, ensuring complete metal coordination. Upon completion of the reaction, the black precipitate was collected by vacuum filtration and washed several times with deionized water to remove any unreacted monomers and anhydrous $FeCl_3$ until the filtrate was colorless. The obtained product was dried at 60 °C under vacuum oven for 12 h, yielding the desired Tp-FeTAPP as a black powder. The synthesis of TP-NiTAPP and TP-(Fe-Ni)TAPP followed a procedure analogous to that of TP-FeTAPP, with anhydrous $FeCl_3$

replaced by $NiCl_2$ for TP-NiTAPP and by an equimolar mixture of anhydrous $FeCl_3$ and $NiCl_2$ for TP-(Fe-Ni)TAPP, respectively.

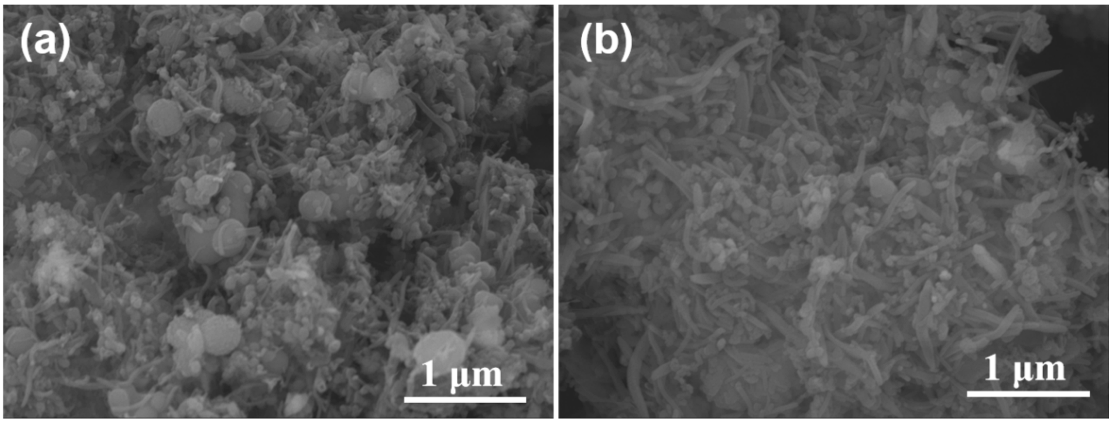

Figure S1. SEM images of (a) Tp-(Fe-Ni)TAPP, and (b) Tp-NiTAPP.

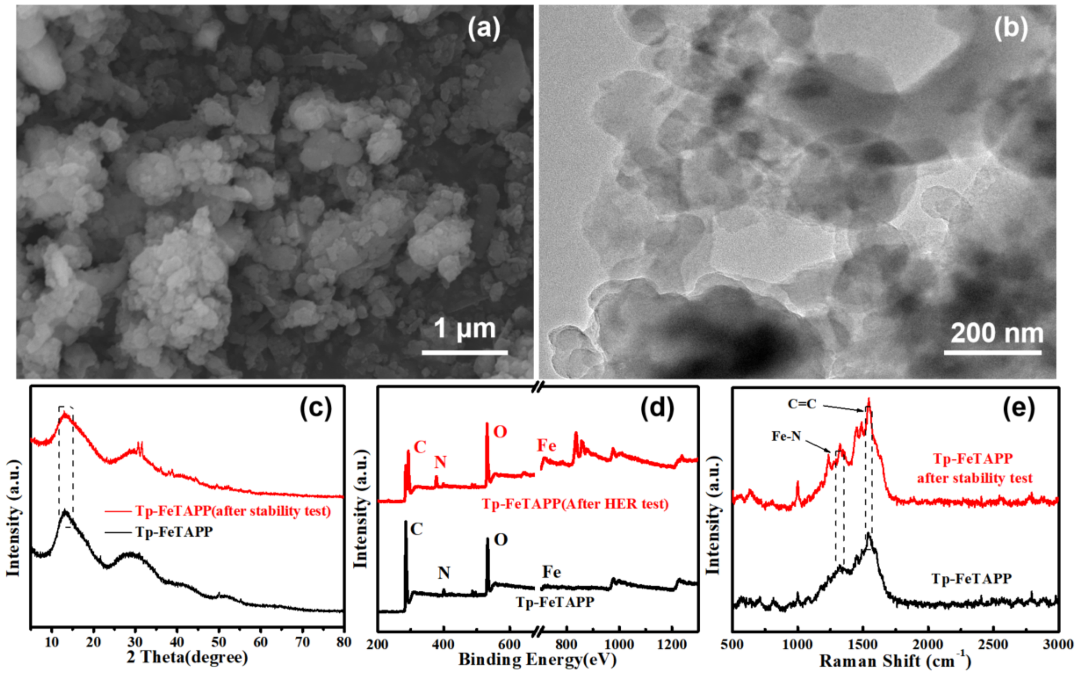

Figure S2. (a) SEM image, (b) TEM image, (c) XRD pattern, (d) XPS and (e) Raman spectra of Tp-FeTAPP after HER test.

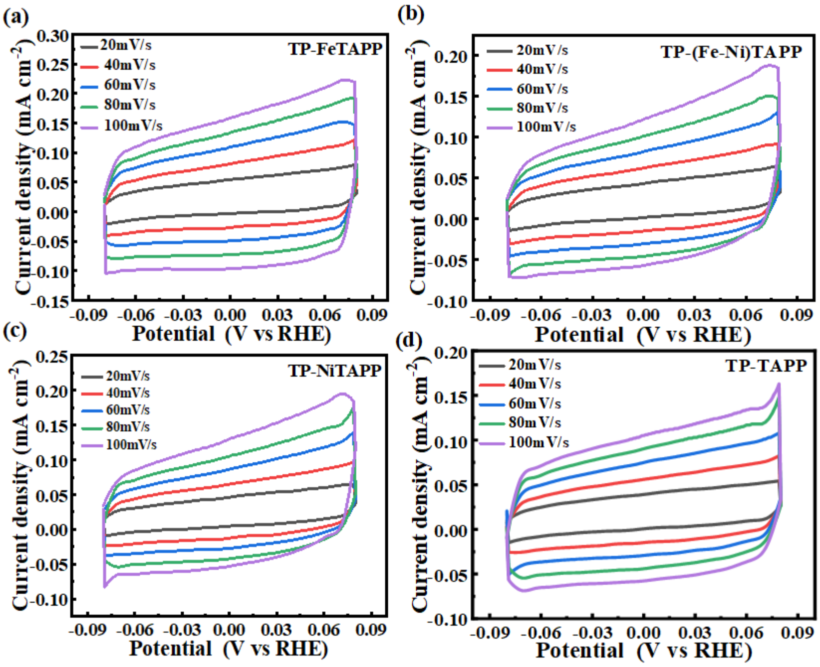

Figure S3. Cyclic voltammetry curves of the samples scanned at different rates from 20 to 100 mV s^{-1} in 1.0 M KOH: (a) Tp-FeTAPP, (b) Tp-(Fe-Ni)TAPP, (c) Tp-NiTAPP, and (d) Tp-TAPP.

Table S1. Comparison of HER performance of **Tp-FeTAPP** with some other reported electrocatalysts at 10 mA cm^{-2}.

Electrocatalysts	**Overpotential (mV@10 mA cm^{-2})**	**Refs.**
GA@Bpy-COF-Co	275 (1.0 M KOH)	[1]
Fe_2O_3/Ni Nanocomposite	163 (1.0 M KOH)	[2]
CoTAPP-CoTNPP	170 (1.0 M KOH)	[3]
CoTPP-PZSNT	157 (1.0 M KOH)	[4]
CoTAPPCC	210 (1.0 M KOH)	[5]
$Nb_4C_3T_x$-180	263 (1.0 M KOH)	[6]
Copper-iron self-supporting electrodes	153 (1.0 M KOH)	[7]
CoTHPP-PDCP@DWCNTs	159 (1.0 M KOH)	[8]
NiFeP@CoCr-LDH	582 (1.0 M KOH)	[9]
NiFe/NF	168 (1.0 M KOH)	[10]
Co_9S_8@MoS_2-2	239 (1.0 M KOH)	[11]
Fe-Ni_5P_4/NiFeOH-350	197 (1.0 M KOH)	[12]
Co_3O_4/MoS_2	205 (1.0 M KOH)	[13]
Tp-FeTAPP	**140 (1.0 M KOH)**	**This work**

References

[1] Z. Wang, J. Li, S. Liu, G. Shao, X. Zhao, A covalent organic framework/graphene aerogel electrocatalyst for enhanced overall water splitting. *Nanoscale* 2022, **14**, 16944-16951.

[2] S. Thangarasu, N. Baby, M. Bhosale, J. Lee, C. Jeong, T.-H. Oh, Fe_2O_3/Ni Nanocomposite Electrocatalyst on Cellulose for Hydrogen Evolution Reaction and Oxygen Evolution Reaction. *Int. J. Mol. Sci.* 2023, **24**, 16282.

[3] Y. Dou, A. Wang, L. Zhao, X. Yang, Q. Wang, M. Shire Sudi, W. Zhu, D. Shang, Boosted hydrogen evolution reaction for a nitrogen-rich azo-bridged metallated porphyrin network. *J. Colloid Interface Sci.* 2023, **650**, 943-950.

[4] X. Yang, W. Zhao, A. Wang, X. Zhai, Y. Dou, K. Syed, W. Zhu, Novel metalloporphyrin covalently functionalized polyphosphazene nanotubes for boosting the hydrogen evolution reaction. *Chem. Commun.* 2024, **60**, 5594-5597.

[5] Y. Dou, X. Yang, Q. Wang, Z. Yang, A. Wang, L. Zhao, W. Zhu, Efficient hydrogen generation of a cobalt porphyrin-bridged covalent triazine polymer. *J. Colloid Interface Sci.* 2023, **644**, 256-263.

[6] Y. Tan, Z. Zhu, X. Zhang, J. Zhang, Y. Zhou, H. Li, H. Qin, Y. Bo, Z. Pan, $Nb_4C_3T_x$ (MXene) as a new stable catalyst for the hydrogen evolution reaction. *Int. J. Hydrogen Energy* 2021, **46**, 1955-1966.

[7] J. Li, C. Han, J. Zhang, P.-F. Yin, X.-W. Du, Copper–Iron Self-Supporting Electrode for Efficient Hydrogen Evolution Reaction. *Langmuir* 2025, **41**, 4730-4735.

[8] X. Yang, X. Zhai, F. Zhang, A. Wang, L. Zhao, W. Zhu, D. Shang, Efficient electrolytic hydrogen evolution from cobalt porphyrin covalently functionalized with chain-like phosphazene on double-walled carbon nanotubes. *J. Colloid Interface Sci.* 2025, **689**, 137238.

[9] R. Zainul, A. B. M. Ali, P. Kanjariya, P. Sharma, R. Thakur, I. Shernazarov, M. Al-Bahrani, A. R. Hussein A. A. Almehizia, NiFeP@CoCr-LDH: A novel bifunctional catalyst for high-performance hydrogen and oxygen evolution reactions. *J. Taiwan Inst. Chem. Eng.* 2025, **169**, 105941.

[10] C. Qin, M. Bai, D. Cao, Y. Ma, J. Zhao, Y. Kang, Z. Zhao, Ultrafast Electrodeposition of Durable NiFe Catalysts for Efficient Hydrogen Evolution Reaction. *ChemistrySelect* 2025, **10** , e202404910.

[11] L. He, S. Huang, Y. Liu, M. Wang, B. Cui, S. Wu, J. Liu, Z. Zhang, M. Du, Multicomponent Co_9S_8@MoS_2 nanohybrids as a novel trifunctional electrocatalyst for efficient methanol electrooxidation and overall water splitting. *J. Colloid Interface Sci.* 2021, **586**, 538-550.

[12] C.-F. Li, J.-W. Zhao, L.-J. Xie, J.-Q. Wu, G.-R. Li, Fe doping and oxygen vacancy modulated Fe-Ni_5P_4/NiFeOH nanosheets as bifunctional electrocatalysts for efficient overall water splitting. *Appl. Catal. B Environ* 2021, **291**, 119987.

[13] A. Muthurasu, V. Maruthapandian, H. Y. Kim, Metal-organic framework derived Co_3O_4/MoS_2 heterostructure for efficient bifunctional electrocatalysts for oxygen evolution reaction and hydrogen evolution reaction. *Appl. Catal. B Environ* 2019, **248**, 202-210.